

Polarized Deeply Inelastic Scattering (DIS) Structure Functions for Nucleons and Nuclei

Ali N. Khorramian ^{a,b,*} S. Atashbar Tehrani ^{b,†} S. Taheri Monfared ^{a,b,‡} F. Arbabifar ^{a,§} and F. I. Olness ^{c¶}

^(a) *Physics Department, Semnan University, Semnan, Iran*

^(b) *School of Particles and Accelerators, Institute for Research in Fundamental Sciences (IPM), P.O.Box 19395-5531, Tehran, Iran*

^(c) *Department of Physics, Southern Methodist University, Dallas, TX 75275-0175, USA*

(Dated: October 13, 2018)

We extract parton distribution functions (PDFs) and structure functions from recent experimental data of polarized lepton-DIS on nucleons at next-to-leading order (NLO) Quantum Chromodynamics. We apply the Jacobi polynomial method to the DGLAP evolution as this is numerically efficient. Having determined the polarized proton and neutron spin structure, we extend this analysis to describe ³He and ³H polarized structure functions, as well as various sum rules. We compare our results with other analyses from the literature.

PACS numbers: 13.60.Hb, 12.39.-x, 14.65.Bt

Contents

I. Introduction	1
II. The Jacobi Polynomial Method	2
III. QCD Analysis & Parametrization	2
A. Parameterization	2
1. First Moments of δu_v and δd_v	3
2. Gluon and Sea-Quarks	3
B. DGLAP Evolution	3
IV. QCD fit of $xg_1(x, Q^2)$ data	3
V. PDF and Structure Function Analysis	4
A. Polarized PDFs	4
B. g_1 Structure Functions	5
C. g_2 Structure Function	6
D. First moment of g_1 structure functions	6
E. Strong Coupling Constant	7
F. Nuclear Polarized Structure Functions	8
G. Bjorken Sum Rule	10
VI. Conclusions	10
Acknowledgments	10
Appendix: FORTRAN-code	10
References	10

I. INTRODUCTION

A fundamental challenge of high energy particle physics is to understand the spin structure of protons, neutrons, and nuclei in terms of their parton constituents. The increasing precision of experimental data on inclusive polarized deeply inelastic scattering (DIS) of leptons from nucleons allows us to perform incisive QCD analyses of polarized structure functions to reveal the spin dependent partonic structure function of the nucleon. Polarized DIS lepton-nucleon scattering experiments have been performed at CERN, SLAC, DESY and JLAB [1–13], and these processes have played a key role in our understanding of QCD and the spin structure of the nucleon [14–18]. There are several comprehensive analyses of the polarized DIS data in the literature [19–44]; this work provides a detailed picture of the spin structure of the nucleons.

The new precision experimental data from the HERMES and COMPASS collaborations [12, 13] of the spin structure function g_1 provides additional information that we shall use to study the spin structure and quark helicity distributions. We shall choose an approach based on the expansion of orthogonal polynomials; specifically, we will implement Jacobi polynomials as we use experimental data for each bin of Q^2 separately [43]. Previously [44], we applied the Jacobi polynomials to determine the polarized valon distributions using only the proton experimental data. In this analysis, both the unpolarized and polarized valon distributions were extracted, so more unknown parameters were required as compared to the present analysis. The Jacobi polynomial expansion has also been applied to a variety of QCD analyses [45–66], including the case of polarized PDFs [44, 67–73].

In the present study, we perform a NLO QCD analysis of the polarized deep-inelastic data [3–13] in the $\overline{\text{MS}}$ -scheme and extract parameterizations of the polarized PDFs and structure functions. In Section II, we provide an overview of the Jacobi polynomials approach. In Section III we review the parametrization and evolution of

*Electronic address: Khorramiana@theory.ipm.ac.ir

†Electronic address: Atashbar@ipm.ir

‡Electronic address: Sara.taherimonfared@gmail.com

§Electronic address: Farbabifar@gmail.com

¶Electronic address: olness@smu.edu

the PDFs. In Section IV we present the results of our fit to the data, and in Section V we compute the associated structure functions and sum rules. Section VI contains the conclusions. We also provide an Appendix which describes the FORTRAN-code which is available.

II. THE JACOBI POLYNOMIAL METHOD

We perform a NLO fit of the polarized parton distributions (PPFDs) using Jacobi polynomials to reconstruct the x dependent quantities from their Mellin moments. The use of Jacobi polynomials has a number of advantages; specifically, it will allow us to factorize the x and Q^2 dependence in a manner that allows an efficient parameterization and evolution of the structure functions.

For example, if we consider the spin structure function $xg_1(x, Q^2)$, we can expand this as:

$$xg_1(x, Q^2) = x^\beta(1-x)^\alpha \sum_{n=0}^{N_{max}} a_n(Q^2) \Theta_n^{\alpha, \beta}(x). \quad (1)$$

Here, $\Theta_n^{\alpha, \beta}(x)$ are Jacobi polynomials of order n , and N_{max} is the maximum order of our expansion. In this instance, the Jacobi polynomials allow us to factor out the essential part of the x -dependence of the structure function into a weight function [45], and the Q^2 -dependence is contained in the Jacobi moments $a_n(Q^2)$.

To be more specific, the x -dependence of the Jacobi polynomials can be written as

$$\Theta_n^{\alpha, \beta}(x) = \sum_{j=0}^n c_j^{(n)}(\alpha, \beta) x^j, \quad (2)$$

where the $c_j^{(n)}(\alpha, \beta)$ coefficients are combinations of Γ -functions involving $\{n, \alpha, \beta\}$. The Jacobi polynomials satisfy an orthogonality relation with weight function $x^\beta(1-x)^\alpha$ as follows:

$$\int_0^1 dx x^\beta(1-x)^\alpha \Theta_k^{\alpha, \beta}(x) \Theta_l^{\alpha, \beta}(x) = \delta_{k,l}. \quad (3)$$

Thus, given the Jacobi moments $a_n(Q^2)$, the polarized structure function $xg_1(x, Q^2)$ may be reconstructed from Eq. (1) [44].

We can compute the Jacobi moments $a_n(Q^2)$ using the orthogonality relation to invert Eq. (1) to obtain:

$$\begin{aligned} a_n(Q^2) &= \int_0^1 dx xg_1(x, Q^2) \Theta_n^{\alpha, \beta}(x) \\ &= \sum_{j=0}^n c_j^{(n)}(\alpha, \beta) \mathbf{M}[xg_1, j+2]. \end{aligned} \quad (4)$$

In Eq. (4), we have substituted Eq. (1) for $xg_1(x, Q^2)$ and introduced the Mellin transform:

$$\mathbf{M}[xg_1, N] \equiv \int_0^1 dx x^{N-2} xg_1(x, Q^2). \quad (5)$$

We can now relate the polarized structure function $xg_1(x, Q^2)$ with its moments [44]

$$\begin{aligned} xg_1(x, Q^2) &= x^\beta(1-x)^\alpha \sum_{n=0}^{N_{max}} \Theta_n^{\alpha, \beta}(x) \\ &\times \sum_{j=0}^n c_j^{(n)}(\alpha, \beta) \mathbf{M}[xg_1, j+2]. \end{aligned} \quad (6)$$

Given Eq. (6) for $xg_1(x, Q^2)$, we choose the set $\{N_{max}, \alpha, \beta\}$ to achieve optimal convergence of this series throughout the kinematic region constrained by the data. In practice, we find $N_{max} = 9$, $\alpha = 3.0$, and $\beta = 0.5$ to be sufficient.

III. QCD ANALYSIS & PARAMETRIZATION

A. Parameterization

We consider a proton comprised of massless partons with helicity distributions $q_\pm(x, Q^2)$ which carry momentum fraction x with a characteristic scale Q . The difference $\delta q(x, Q^2) = q_+(x, Q^2) - q_-(x, Q^2)$ measures how much the parton of flavor q ‘‘remembers’’ of the parent proton polarization. We will parameterize these polarized PDFs at initial scale $Q_0^2 = 4 \text{ GeV}^2$ using the following form:

$$x \delta q(x, Q_0^2) = \mathcal{N}_q \eta_q x^{a_q} (1-x)^{b_q} (1+c_q x), \quad (7)$$

where the polarized PDFs are determined by parameters $\{\eta_q, a_q, b_q, c_q\}$, and the generic label $q = \{u_v, d_v, \bar{q}, g\}$ denotes the partonic flavors up-valence, down-valence, sea, and gluon, respectively. The normalization constants \mathcal{N}_q

$$\frac{1}{\mathcal{N}_q} = \left(1 + c_q \frac{a_q}{a_q + b_q + 1} \right) B(a_q, b_q + 1), \quad (8)$$

are chosen such that η_i are the first moments of $\delta q_i(x, Q_0^2)$, $\eta_i = \int_0^1 dx \delta q_i(x, Q_0^2)$, where $B(a, b)$ is the Euler beta function.

The total up and down PDFs are a sum of the valence plus sea distributions: $\delta u = \delta u_v + \delta \bar{q}$ and $\delta d = \delta d_v + \delta \bar{q}$. We will assume an $SU(3)$ flavor symmetry such that $\delta \bar{q} \equiv \delta \bar{u} = \delta \bar{d} = \delta s = \delta \bar{s}$. While we could allow for an $SU(3)$ symmetry violation term by introducing κ such that $\delta s = \delta \bar{s} = \kappa \delta \bar{q}$, as the strange PDF is poorly constrained the results would be insensitive to the specific choice of κ .

As seen from Eq. (7), each of four polarized parton densities $q = \{u_v, d_v, \bar{q}, g\}$ contain four parameters $\{\eta_q, a_q, b_q, c_q\}$ which gives a total of 16 parameters that we must constrain. We now demonstrate that we can eliminate some of these parameters while maintaining sufficient flexibility to obtain a good fit.

1. First Moments of δu_v and δd_v

The parameters η_{u_v} and η_{d_v} are the first moments of the δu_v and δd_v polarized valence quark densities; these quantities can be related to F and D as measured in neutron and hyperon β -decays according to the relations [74]:

$$a_3 = \int_0^1 dx \delta q_3 = \eta_{u_v} - \eta_{d_v} = F + D, \quad (9)$$

$$a_8 = \int_0^1 dx \delta q_8 = \eta_{u_v} + \eta_{d_v} = 3F - D. \quad (10)$$

where a_3 and a_8 are non-singlet combinations of the first moments of the polarized parton densities corresponding to

$$q_3 = (\delta u + \delta \bar{u}) - (\delta d + \delta \bar{d}), \quad (11)$$

$$q_8 = (\delta u + \delta \bar{u}) + (\delta d + \delta \bar{d}) - 2(\delta s + \delta \bar{s}). \quad (12)$$

A reanalysis of F and D with updated β -decay constants obtained [74] $F = 0.464 \pm 0.008$ and $D = 0.806 \pm 0.008$. With these values we find:

$$\eta_{u_v} = +0.928 \pm 0.014, \quad (13)$$

$$\eta_{d_v} = -0.342 \pm 0.018. \quad (14)$$

We make use of η_{u_v} and η_{d_v} to reduce the number of parameters by two.

2. Gluon and Sea-Quarks

We find the factor $(1 + c_q x)$ in Eq. (7) provides flexibility to obtain a good description of the data, particularly for the valence distributions $\{u_v, d_v\}$. Thus we will make use of the c_q coefficients for the the up-valence and down-valence distributions; in contrast, we are able to set the values for $c_{\bar{q}}$ and c_g to zero ($c_{\bar{q}} = c_g = 0$) while maintaining a good fit and eliminating two free parameters. For the parameters $\{c_{u_v}, c_{d_v}\}$ we find the fit improves if we use non-zero values, but as these are relatively flat directions in χ -space we shall fix the values as detailed in Table I.

Separately, we find the b parameters control the large- x behavior of the PDFs; thus, the sea-quark and gluon distributions have large uncertainties in this region as they are dominated by the valence. To provide some guidance, we observe that for *unpolarized* parton densities in the large- x region, a ratio of $b_{\bar{q}}/b_g \sim 1.6$ provides a good fit. Therefore we impose this ratio on the *polarized* $b_{\bar{q}}$ and b_g parameters to further reduce the free parameters. Additionally, we are able to extract reasonable constraints on the $a_{\bar{q}}$ and a_g parameters; this is a benefit of the Jacobi polynomials.

Having fixed $\{\eta_{u_v}, \eta_{d_v}, c_{\bar{q}}, c_g\}$ and the ratio $b_{\bar{q}}/b_g$ in preliminary minimization, we then set the parameters

$\{b_{\bar{q}}, b_g, c_{u_v}, c_{d_v}\}$ as indicated in Table I; this gives us a total of 9 unknown parameters, in addition to $\alpha_s(Q_0^2)$.

B. DGLAP Evolution

In the Jacobi polynomial approach the DGLAP evolution equations are solved in Mellin space. The Mellin transform of the parton densities q are defined analogous to that of Eq. (5):

$$\begin{aligned} \mathbf{M}[\delta q(x, Q_0^2), N] &\equiv \delta q(N, Q_0^2) = \int_0^1 x^{N-1} \delta q(x, Q_0^2) dx \\ &= \mathcal{N}_q \eta_q \left(1 + c_q \frac{N-1+a_q}{N+a_q+b_q} \right) \\ &\times B(N-1+a_q, b_q+1), \end{aligned} \quad (15)$$

where $q = \{u_v, d_v, \bar{q}, g\}$, and B is the Euler beta function.

In Mellin space, the twist-2 contributions to the polarized structure function $g_1(N, Q^2)$ can be represented in terms of the polarized parton densities and the coefficient functions ΔC_i^N by:

$$\begin{aligned} \mathbf{M}[g_1^p, N] &= \frac{1}{2} \sum_q e_q^2 \left\{ \left(1 + \frac{\alpha_s}{2\pi} \Delta C_q^N \right) \right. \\ &\times [\delta q(N, Q^2) + \delta \bar{q}(N, Q^2)] \\ &\left. + \frac{\alpha_s}{2\pi} 2\Delta C_g^N \delta g(N, Q^2) \right\}. \end{aligned} \quad (16)$$

Here, the sum runs over quark flavors $\{u, d, s\}$, and $\{\delta q, \delta \bar{q}, \delta g\}$ are the polarized quark, anti-quark, and gluon distributions, respectively.

The coefficient functions ΔC_i^N are the N -th moments of spin-dependent Wilson coefficients, and are given by [16]:

$$\begin{aligned} \Delta C_q^N &= \frac{4}{3} \left\{ -S_2(N) + (S_1(N))^2 + \left(\frac{3}{2} - \frac{1}{N(N+1)} \right) \right. \\ &\times \left. S_1(N) + \frac{1}{N^2} + \frac{1}{2N} + \frac{1}{N+1} - \frac{9}{2} \right\}, \\ \Delta C_g^N &= \frac{1}{2} \left[-\frac{N-1}{N(N+1)} (S_1(N) + 1) - \frac{1}{N^2} + \frac{2}{N(N+1)} \right], \end{aligned}$$

with $S_1(n) = \sum_{j=1}^n \frac{1}{j} = \psi(n+1) + \gamma_E$, $S_2(n) = \sum_{j=1}^n \frac{1}{j^2} = \left(\frac{\pi^2}{6} \right) - \psi'(n+1)$, $\psi(n) = \Gamma'(n)/\Gamma(n)$ and $\psi'(n) = d^2 \ln \Gamma(n)/dn^2$.

In summary, we are able to express xg_1^p in terms of 9 unknown parameters at an input scale of $Q_0^2 = 4 \text{ GeV}^2$. We now examine the fits to the spin structure functions to extract the polarized PDFs from the available data.

IV. QCD FIT OF $xg_1(x, Q^2)$ DATA

Our analysis is performed using the QCD-PEGASUS program [75]. We work at NLO in the QCD evolution

	η_{u_v}	0.928 (<i>fixed</i>)		$\eta_{\bar{q}}$	-0.054 ± 0.029
δu_v	a_{u_v}	0.535 ± 0.022	$\delta \bar{q}$	$a_{\bar{q}}$	0.474 ± 0.121
	b_{u_v}	3.222 ± 0.085		$b_{\bar{q}}$	9.310 (<i>fixed</i>)
	c_{u_v}	8.180 (<i>fixed</i>)		$c_{\bar{q}}$	0
δd_v	η_{d_v}	-0.342 (<i>fixed</i>)		η_g	0.224 ± 0.118
	a_{d_v}	0.530 ± 0.067	δg	a_g	2.833 ± 0.528
	b_{d_v}	3.878 ± 0.451		b_g	5.747 (<i>fixed</i>)
	c_{d_v}	4.789 (<i>fixed</i>)		c_g	0
$\alpha_s(Q_0^2) = 0.381 \pm 0.017$					
$\chi^2/dof = 273.6/370 = 0.74$					

Table I: Final parameter values and their statistical errors in the $\overline{\text{MS}}$ -scheme at the input scale $Q_0^2 = 4 \text{ GeV}^2$.

using $N_f = 3$ in the fixed-flavor number scheme with massless partonic flavors $\{u, d, s\}$. We take the renormalization and factorization scales to be equal ($\mu_R = \mu_F$), and we compute the strong coupling $\alpha_s(Q^2)$ at NLO using a fourth order Runge-Kutta integration. Our initial parameterizations (Eq. 7) are chosen to be invertible in N-space, and this makes our fitting procedure numerically efficient.

For the proton data we use EMC [3], HERMES [5, 12], SMC [8], E143 [9], E155 [11] and COMPASS [13], for the neutron data we use E142[4], HERMES [5, 12] and E154 [6, 7], and for the deuteron data we use SMC [8], E143 [9], E155 [10] and HERMES[12]. This data is summarized in Table II.

We minimize the global χ^2 [63, 66, 76]:

$$\chi_{\text{global}}^2 = \sum_n w_n \chi_n^2, \quad (17)$$

where the sum n runs over the different experiments, w_n is a weight factor for the n -th experiment, and χ_n^2 is given by:

$$\chi_n^2 = \left(\frac{1 - \mathcal{N}_n}{\Delta \mathcal{N}_n} \right)^2 + \sum_i \left(\frac{\mathcal{N}_n g_{1,i}^{\text{exp}} - g_{1,i}^{\text{theor}}}{\mathcal{N}_n \Delta g_{1,i}^{\text{exp}}} \right)^2. \quad (18)$$

Here, $g_{1,i}^{\text{exp}}$, $\Delta g_{1,i}^{\text{exp}}$, and $g_{1,i}^{\text{theor}}$ denote the experimental measurement, the experimental uncertainty (statistical and systematic combined in quadrature) and theoretical value for the i^{th} data point, respectively. $\Delta \mathcal{N}_n$ is the experimental normalization uncertainty and \mathcal{N}_n is an overall normalization factor for the data of experiment n . We allow for a relative normalization shift \mathcal{N}_n between different data sets within uncertainties $\Delta \mathcal{N}_n$ quoted by the experiments.

We minimize the above χ^2 value with the 9 unknown parameters plus an undetermined $\alpha_s(Q_0^2)$. The values of these parameters are summarized in Table I. We find $\chi^2/d.o.f. = 273.6/370$ which yields an acceptable fit to the experimental data.

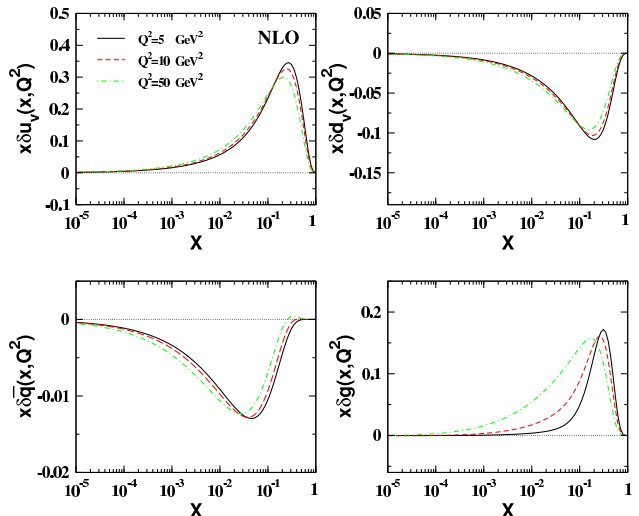


Figure 1: The polarized parton distribution as function of x and for different values of Q^2 .

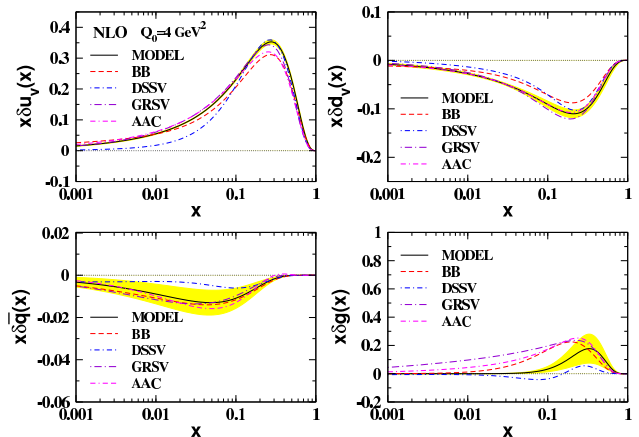


Figure 2: The polarized parton distribution at $Q_0^2 = 4 \text{ GeV}^2$ as a function of x . Our fit is the solid curve. Also shown are the results of BB (dashed) [40], DSSV (dashed-dotted) [38], GRSV (long dashed-dotted) [28], and AAC (dashed-dashed-dotted) [39].

V. PDF AND STRUCTURE FUNCTION ANALYSIS

We next present our polarized PDFs and perform comparisons with other recent parameterizations [28, 31–34].

A. Polarized PDFs

Figure 1 displays our polarized PDFs for a selection of Q^2 values. The up-valence ($x\delta u_v$) and gluon ($x\delta g$) distributions are positive, while the down-valence ($x\delta d_v$) and sea ($x\delta \bar{q}$) distributions are negative. We observe that the evolution shifts all the distributions to smaller values of

Experiment	x -range	Q^2 -range[GeV ²]	# of data points	\mathcal{N}_i
E143 (p)	0.031-0.749	1.27-9.52	28	0.9998
HERMES (p)	0.028-0.66	1.01-7.36	39	1.0006
SMC (p)	0.005-0.480	1.30-58.0	12	0.9999
EMC (p)	0.015-0.466	3.50-29.5	10	1.0094
E155	0.015-0.750	1.22-34.72	24	1.0226
HERMES06 (p)	0.026-0.731	1.12-14.29	51	0.9992
COMPASS10 (p)	0.005-0.568	1.10-62.10	15	0.9920
Proton			179	
E143 (d)	0.031-0.749	1.27-9.52	28	0.9990
E155 (d)	0.015-0.750	1.22-34.79	24	0.9998
SMC (d)	0.005-0.479	1.30-54.80	12	0.9999
HERMES06 (d)	0.026-0.731	1.12-14.29	51	0.9976
Deuteron			115	
E142 (n)	0.035-0.466	1.10-5.50	8	0.9991
HERMES (n)	0.033-0.464	1.22-5.25	9	0.9999
E154 (n)	0.017-0.564	1.20-15.00	17	0.9996
HERMES06 (n)	0.026-0.731	1.12-14.29	51	1.0000
Neutron			85	
Total			379	

Table II: Published data points with the measured x and Q^2 ranges, the number of data points (with a cut of $Q^2 \geq 1.0$ GeV²), and the fitted normalization shifts \mathcal{N}_i .

x , and tends to flatten out the peak for increasing Q^2 . Figure 2 displays the extracted NLO polarized PDFs as compared with various parameterizations from the literature [28, 38–40].

Examining the $x\delta u_v$ and $x\delta\bar{q}$ distributions we see that most of the fits are in agreement, with the possible exception of the DSSV [38] curves; for both distributions, the DSSV results approach zero more quickly than the other curves. For the $x\delta d_v$ distribution, all of the curves are comparable. The DSSV analysis employs results from semi-inclusive DIS (SI-DIS) data which can impose individual constraints on individual quark flavor distributions in the nucleon [38]. Finally, for the gluon distribution, the DSSV results have a sign change in the region of $x \sim 0.1$ while the other fits are positive. Our result for gluon distribution is located between DSSV curve and the other fits [28, 39, 40]. In particular, we find the gluon polarization vanished more quickly for small x values as compared with the other fits; we conjecture that using available asymmetry data in low x region may contribute to this difference.

B. g_1 Structure Functions

Figure 3 displays results for the polarized structure function xg_1^p . For comparison, we display the results obtained by (Blumlein, Bottcher) BB [31], (Gluck, Reya, Stratmann, Vogelsang) GRSV [28], (Leader, Sidorov, Stamenov) LSS [34], (de Florian, Navarro, Sassot) DNS [33] and (Asymmetry Analysis Collaboration) AAC [32]. There is some spread in the analyses at low values of x ; however, the data are generally well described within errors. As in the unpolarized case, the presence of scaling violations result a slope that varies with changing x val-

ues; this is evident in Figure 3 where we observe the Q^2 dependence of the structure function $g_1(x, Q^2)$.

Given the polarized proton PDFs, we can use isospin symmetry to obtain the corresponding neutron structure functions. In Figure 4, we plot the neutron polarized structure function xg_1^n . We also display the NLO QCD curves obtained by Ref. [44] in the polarized valon model (PVM).

We can relate the deuteron structure function to that of the proton and neutron via:

$$\mathbf{M}[g_1^d, N] = \frac{1}{2} \left(1 - \frac{3}{2} \omega_D\right) (\mathbf{M}[g_1^p, N] + \mathbf{M}[g_1^n, N]) , \quad (19)$$

where $\omega_D = 0.05 \pm 0.01$ is the D -state wave probability for the deuteron [77]. In Figure 5 we present our results for the structure functions $xg_1^p(x, Q^2)$, $xg_1^n(x, Q^2)$ and $xg_1^d(x, Q^2)$, and this compares favorably with the results of the BB [31], GRSV [28], LSS [34], DNS [33] and AAC [32] analyzes.

The non-singlet spin structure function $xg_1^{NS}(x, Q^2)$ is defined as [12]

$$\begin{aligned} xg_1^{NS}(x, Q^2) &\equiv xg_1^p(x, Q^2) - xg_1^n(x, Q^2) \\ &= 2[xg_1^p(x, Q^2) - \frac{xg_1^d(x, Q^2)}{1 - \frac{3}{2}\omega_D}] . \quad (20) \end{aligned}$$

This is displayed in Figure 6, and we compare with the HERMES data [12] for various Q^2 bins. In the second line of Eq. (20) we have related the structure function of the deuteron using isospin symmetry and the relation of Eq. (19).

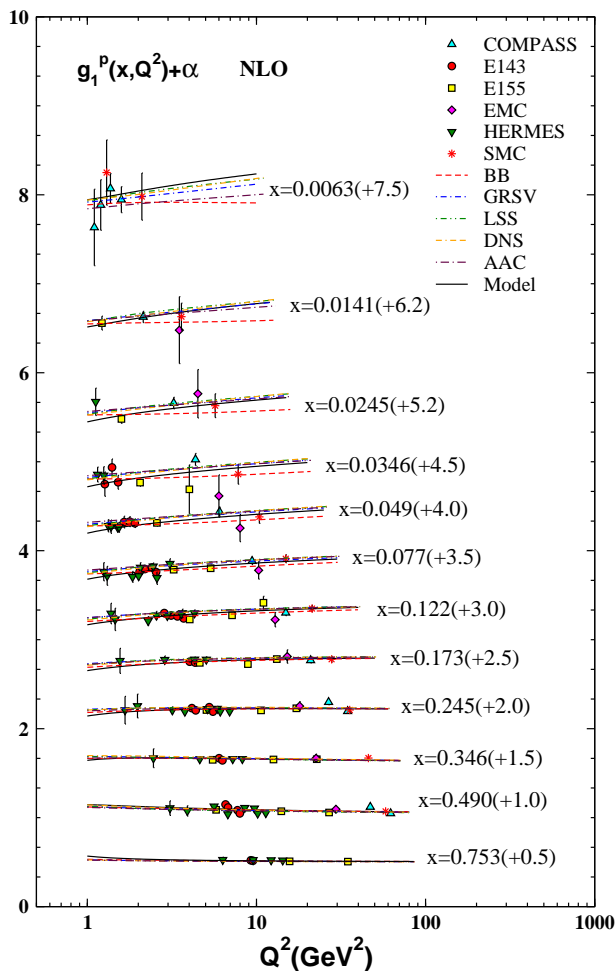


Figure 3: The polarized structure function g_1^p as function of Q^2 in intervals of x . The error bars shown are the statistical and systematic uncertainties added in quadrature. Our fit is the solid curve. The values of the shift α are given in parentheses. Also shown are the results of BB (dashed) [31], GRSV (dashed-dotted) [28], LSS (dashed-dotted-dotted) [34], DNS (dashed-dashed-dotted) [33] and AAC (long dashed-dotted) [32].

C. g_2 Structure Function

We can now extract the structure function xg_2 via the Wandzura-Wilczek relation [78, 79]:

$$g_2(x, Q^2) = -g_1^p(x, Q^2) + \int_x^1 \frac{dy}{y} g_1^p(y, Q^2). \quad (21)$$

This relation remains valid in the presence of target mass corrections. In Figure 7 we show our result for xg_2 and we compare it with the experimental data from E143 [9] and SMC [8].

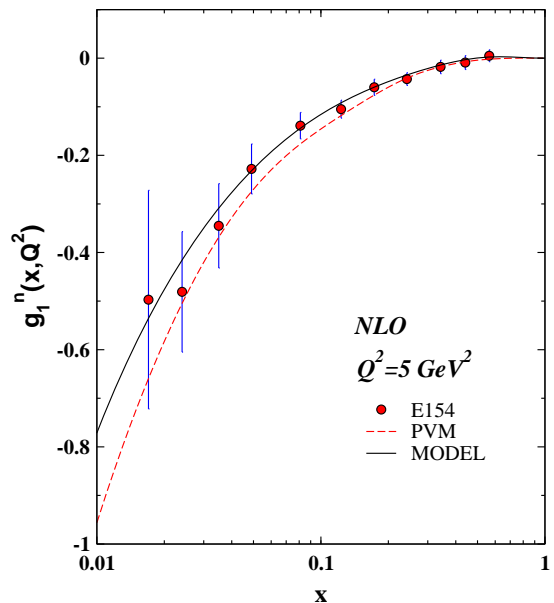


Figure 4: The polarized structure function xg_1^n as function of x and for a fixed value of $Q^2 = 5 \text{ GeV}^2$. The present fit is the solid curve. Also shown are the results of AK [44] (dashed) according to polarized valon model (PVM).

Q^2	2 GeV^2	3 GeV^2	5 GeV^2	10 GeV^2
Δu_v	0.928864	0.928310	0.927794	0.927288
Δd_v	-0.342318	-0.342114	-0.341924	-0.341738
$\Delta \bar{q}$	-0.053400	-0.053893	-0.054379	-0.054789
Δg	0.143610	0.191313	0.248845	0.323886
Γ_1^p	0.128291	0.131199	0.133822	0.136303
Γ_1^n	-0.050972	-0.052416	-0.053735	-0.055000
Γ_1^d	0.035296	0.035965	0.036559	0.037115

Table III: The first moments of polarized parton distributions, Δu_v , Δd_v , $\Delta \bar{q}$, Δg and polarized structure functions Γ_1^p , Γ_1^n , Γ_1^d in NLO in the $\overline{\text{MS}}$ -scheme for some different values of Q^2 .

D. First moment of g_1 structure functions

We next use the polarized PDFs to compute the first moments, and compare with other recent analyzes. We can obtain the first moment of g_1^p by

$$\Gamma_1^p(Q^2) \equiv \int_0^1 dx g_1^p(x, Q^2). \quad (22)$$

The results of our fit are presented in Table III for selected values of Q^2 , and these are compared with results from the literature in Table IV.

In the framework of QCD the spin of the proton can be expressed in terms of the first moment of the total quark and gluon helicity distributions and their orbital angular momentum, i.e.

$$\frac{1}{2} = \frac{1}{2} \Delta \Sigma^p + \Delta g^p + L_z^p, \quad (23)$$

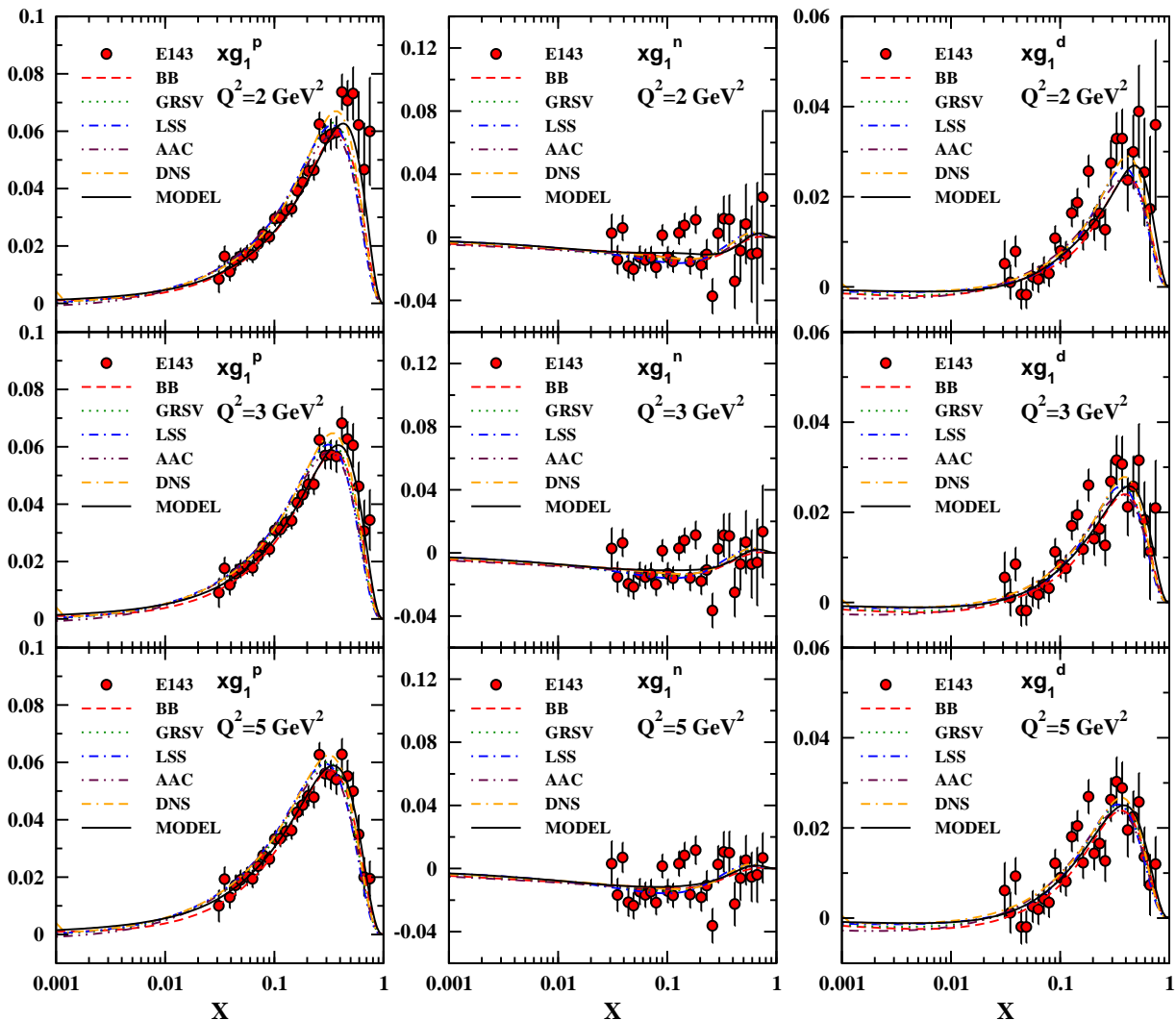


Figure 5: The polarized structure function xg_1^p , xg_1^n and xg_1^d as a function of x for selected values of Q^2 . The data are well described by the fit (solid curve). Also shown are the QCD NLO curves obtained by BB (dashed) [31], GRSV (dotted) [28], LSS (dashed-dotted) [34], AAC (dashed-dotted-dotted) [32] and DNS (dashed-dashed-dotted) [33].

	Model	BB [40]	GRSV [28]	AAC [32]
Δu_v	0.928	0.928	0.9206	0.9278
Δd_v	-0.342	-0.342	-0.3409	-0.3416
Δu	0.874	0.866	0.8593	0.8399
Δd	-0.396	-0.404	-0.4043	-0.4295
$\Delta \bar{q}$	-0.054	-0.062	-0.0625	-0.0879
Δg	0.224	0.462	0.6828	0.8076

Table IV: Comparison of the first moments of the polarized parton densities in NLO in the $\overline{\text{MS}}$ -scheme at $Q^2 = 4 \text{ GeV}^2$ for different sets of recent parton parameterizations. The second column (Model) contains the first moments which is obtained from our new parametrization based on the Jacobi polynomials expansion method. The BB [40], GRSV [28] and AAC [32] results are also shown.

where L_z^p is the total orbital angular momentum of all quarks and gluons. The contribution of $\frac{1}{2}\Delta\Sigma + \Delta g$ for

typical value of $Q^2 = 4 \text{ GeV}^2$ is around 0.355 in our analysis. We can also compare this value in NLO with other recent analysis. The reported value from the BB model [40] is 0.569, the AAC model [32] is 0.837 and the GRSV model [28] is 0.785, while the DSSV model [38] is approximately 0.1. Since the values of $\frac{1}{2}\Delta\Sigma$ are comparable, we observe that the difference between the above reported values must come from different gluon distributions.

E. Strong Coupling Constant

In this QCD analysis we extract $\alpha_s(Q_0^2)$ at NLO and obtain

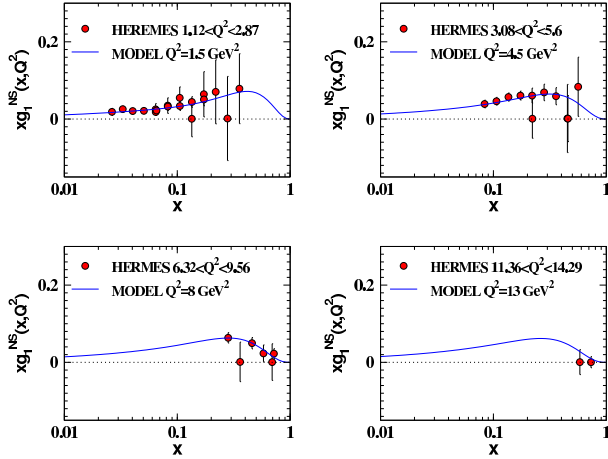


Figure 6: The non-singlet polarized structure function xg_1^{NS} as function of x .

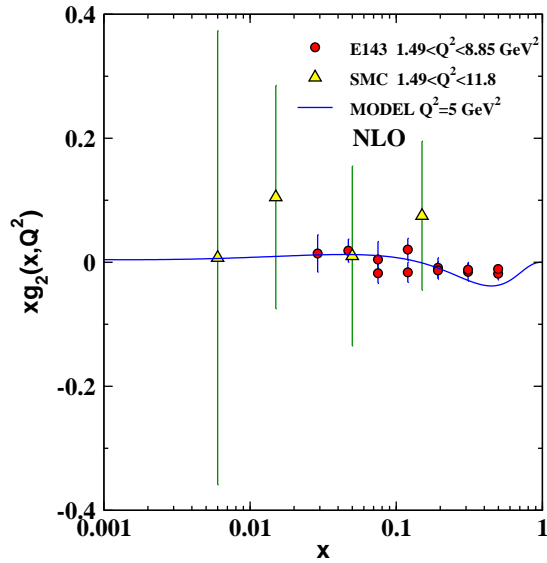


Figure 7: The polarized structure function xg_2 as function of x for $Q^2 = 5 \text{ GeV}^2$.

$$\alpha_s(Q_0^2) = 0.381 \pm 0.017. \quad (24)$$

Rescaling this to the Z boson mass scale we find

$$\alpha_s(M_Z^2) = 0.1149 \pm 0.0015. \quad (25)$$

The error given in above does not include the relative systematics of the different classes of measurements. In Table V we provide a comparison of this value with other determinations from the literature computed at NLO and higher orders, including the current world average of $\alpha_s(M_Z^2) = 0.1184 \pm 0.0007$.

$\alpha_s(M_Z^2)$	Order	Reference	Notes
0.1149 ± 0.0015	NLO		This analysis
$0.1132^{+0.0056}_{-0.0095}$	NLO	[40]	
$0.1134^{+0.0019}_{-0.0021}$	NNLO	[80]	
0.1141 ± 0.0036	NLO	[44]	
0.1131 ± 0.0019	NNLO	[63]	
0.1139 ± 0.0020	NNNLO	[66]	
$0.1141^{+0.0020}_{-0.0022}$	NNNLO	[80]	
0.1135 ± 0.0014	NNLO	[81]	FFS
0.1129 ± 0.0014	NNLO	[81]	BSMN
0.1124 ± 0.0020	NNLO	[82]	dynamic approach
0.1158 ± 0.0035	NNLO	[82]	standard approach
0.1171 ± 0.0014	NNLO	[83]	
0.1147 ± 0.0012	NNLO	[84]	
0.1145 ± 0.0042	NNLO	[85]	(Preliminary)
0.1184 ± 0.0007	—	[86]	World Average

Table V: Comparison of $\alpha_s(M_Z)$ values from the literature.

n	p	
$a^n = 5.650556817$	$a_0^p = 0.0148376$	$b_0^p = 4.15388$
$b^n = 0.986818274$	$a_1^p = -0.0189575$	$b_1^p = -4.75525$
$c^n = 0.064446823$	$a_2^p = 0.0121792$	$b_2^p = 2.68417$
$d^n = 0.807650292$	$a_3^p = -0.0040397$	$b_3^p = -0.800306$
	$a_4^p = 0.000540845$	$b_4^p = 0.101095$

Table VI: Numerical coefficients for Eqs. (28,29) of $\Delta f_{3He}^n(y)$ and $\Delta f_{3He}^p(y)$ obtained from Refs. [88–90].

F. Nuclear Polarized Structure Functions

Using the polarized PDF fit results, we examine the nucleon corrections factors for ${}^3\text{He}$ and ${}^3\text{H}$. The polarized structure functions g_1^{3He} and g_1^{3H} can be composed from the polarized proton structure g_1^p and the polarized neutron structure g_1^n as follows:

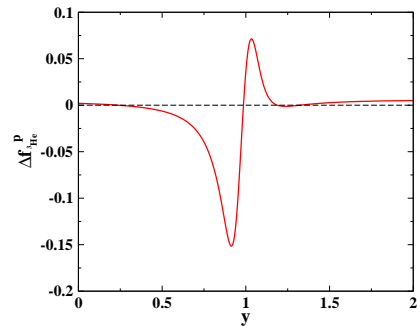


Figure 8: The polarized light cone distribution function for the proton in the ${}^3\text{He}$, based on the results of Ref. [88–90].

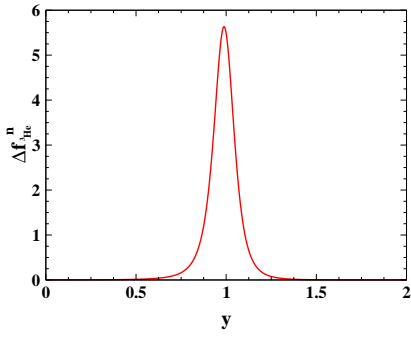


Figure 9: The polarized light cone distribution function for the neutron in the ${}^3\text{He}$, based on the results of Ref. [88–90].

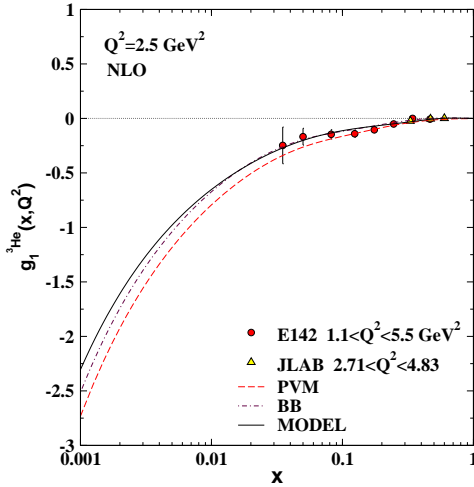


Figure 10: Analytical result for the polarized ${}^3\text{He}$ structure function *v.s.* x for fixed $Q^2 = 2.5 \text{ GeV}^2$. The current fit is the solid curve. Also shown are the QCD NLO curves obtained by AK (dashed) [44] according to polarized valon model (PVM) and BB (dashed-dotted) [31].

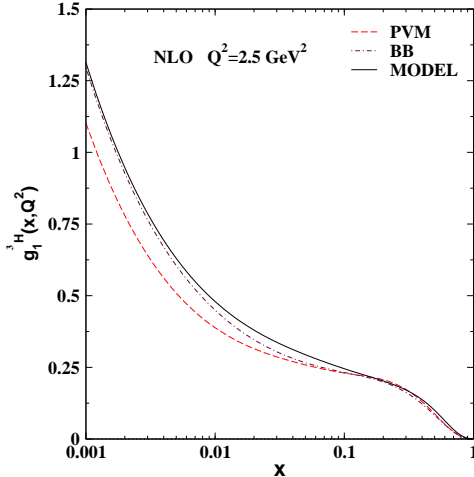


Figure 11: Analytical result for the polarized ${}^3\text{H}$ structure function *v.s.* x for fixed $Q^2 = 2.5 \text{ GeV}^2$. The current fit is the solid curve. Also shown are the QCD NLO curves obtained by AK (dashed) [44] according to polarized valon model (PVM) and BB (dashed-dotted) [31] for comparison.

$$g_1^{3He}(x, Q^2) = \int_x^3 \frac{dy}{y} \Delta f_{3He}^n(y) g_1^n\left(\frac{x}{y}, Q^2\right) + 2 \int_x^3 \frac{dy}{y} \Delta f_{3He}^p(y) g_1^p\left(\frac{x}{y}, Q^2\right) - 0.014[g_1^p(x, Q^2) - 4g_1^n(x, Q^2)], \quad (26)$$

$$g_1^{3H}(x, Q^2) = 2 \int_x^3 \frac{dy}{y} \Delta f_{3H}^n(y) g_1^n\left(\frac{x}{y}, Q^2\right) + \int_x^3 \frac{dy}{y} \Delta f_{3H}^p(y) g_1^p\left(\frac{x}{y}, Q^2\right) + 0.014[g_1^p(x, Q^2) - 4g_1^n(x, Q^2)]. \quad (27)$$

Here, $\Delta f_{3He}^N(y)$ and $\Delta f_{3H}^N(y)$ are the spin-dependent nucleon light-cone momentum distributions [87, 88]. These functions parameterize the Fermi motion and the nucleon binding, and are readily calculated using the ground-state wave functions of ${}^3\text{He}$ and ${}^3\text{H}$. Note that the last term in above equations is important only in the large- x region.

If we utilize isospin symmetry, we can equate $\Delta f_{3He}^p(y)$ to $\Delta f_{3H}^n(y)$, and also $\Delta f_{3He}^n(y)$ to $\Delta f_{3H}^p(y)$; thus, we are left with only two independent functions $\Delta f_{3He}^p(y)$ and $\Delta f_{3He}^n(y)$. Using the results of Refs. [88–90], we express these distributions as

$$\Delta f_{3He}^n(y) = \frac{a^n e^{-\frac{0.5(1-d^n)(-b^n+y)^2}{(c^n)^2}}}{1 + \frac{d^n(-b^n+y)^2}{(c^n)^2}}, \quad (28)$$

$$\Delta f_{3He}^p(y) = \frac{\sum_{i=0}^4 a_i^p U_i(y)}{\sum_{i=0}^4 b_i^p U_i(y)}, \quad (29)$$

where $U_n(y)$ is a Chebyshev polynomials of the second type. The numerical coefficients of these equations are presented in Table VI. We can then use Eqs. (26,27) to obtain the polarized nucleon structure functions $g_1^{3He}(x, Q^2)$ and $g_1^{3H}(x, Q^2)$.

To determine the g_1^{3He} and g_1^{3H} polarized structure functions we need the polarized light-cone distribution functions for proton and neutron in ${}^3\text{He}$, i.e. Δf_{3He}^p and Δf_{3He}^n . In Figures 8 and 9 we present our results using the parametrization of Eqs. (28,29) which is based on the numerical results of Ref. [90].

In Figures 10 and 11 we show our results for the g_1^{3He} and g_1^{3H} polarized structure function, and compare with BB [31], and the polarized valon model (PVM) [44]. For the g_1^{3He} polarized structure function we see that our result coincides with the BB fit for x values down to $\sim 10^{-2}$, and then falls off more quickly at very small x values. The polarized valon model (PVM), while still a reasonable fit to the data, lies below both of the other

fits. For the g_1^{3H} polarized structure function, our fit coincides with the BB fit at both large and small x values, but dips below it (closer to the PVM) for intermediate x values. The differences between these curves come from the various data sets used, the constraints imposed, and the form of the parameterization. For example, in the AK fit [44], only 257 experimental data points were used as the neutron data were not included; in contrast, the present analysis uses 379 points which does include the neutron data. Furthermore, the AK fit used 15 free parameters while there are only 9 free parameters in the present analysis. These differences are reflected in the extractions of PPDFs, and a comparison of these different analyses may be indicative of the stability of the determined QCD parameters.

G. Bjorken Sum Rule

We can also study the Bjorken sum rule [91] which relates the difference of the first moments of the proton and neutron spin structure functions to the axial vector coupling constant of the neutron β -decay,

$$\int_0^1 [g_1^p(x, Q^2) - g_1^n(x, Q^2)] dx = \frac{1}{6} g_A [1 + O(\frac{\alpha_s}{\pi})], \quad (30)$$

where $g_A = 1.2670 \pm 0.0035$ [74], and the QCD radiative corrections are denoted as $O(\frac{\alpha_s}{\pi})$. This sum rule can be generalized for the ${}^3\text{He}$ - ${}^3\text{H}$ system as follows:

$$\int_0^3 [g_1^{3H}(x, Q^2) - g_1^{3He}(x, Q^2)] dx = \frac{1}{6} \tilde{g}_A [1 + O(\frac{\alpha_s}{\pi})], \quad (31)$$

where \tilde{g}_A is the axial vector coupling constant of the Triton β -decay, with $\tilde{g}_A = 1.211 \pm 0.002$ [92]. Taking the ratio of the Eqs. (30) and (31), we find

$$\frac{\int_0^3 [g_1^{3H}(x, Q^2) - g_1^{3He}(x, Q^2)] dx}{\int_0^1 [g_1^p(x, Q^2) - g_1^n(x, Q^2)] dx} = \frac{\tilde{g}_A}{g_A}. \quad (32)$$

Given g_A and \tilde{g}_A , we compute the above ratio to be 0.956 [88]. Note that the QCD radiative corrections are expected to cancel exactly in above equation. Using the Bjorken sum rules of Eqs. (30,31), we obtain the value 0.924 for the ratio of Eq. (32).

VI. CONCLUSIONS

We have presented a fit to the polarized lepton-DIS data on nuclei at NLO QCD using the Jacobi polynomial method.

Having extracted the polarized PDFs, we compute various nuclear structure functions (g_1, g_2) and Bjorken sum rule. In general, we find good agreement with the experimental data, and our results are in accord with other determinations from the literature; collectively, this demonstrates progress of the field toward a detailed description of the spin structure of the nucleon.

Having demonstrated the compatibility of the Jacobi polynomial method with other approaches in the literature, this study can serve as a foundation for addressing issues of polarized scattering processes from a complementary perspective. In particular, the Jacobi polynomial method offers the opportunity to examine efficiencies of different methods, and this work is in progress.

Acknowledgments

We thank S. Kumano and M. Miyama of the ACC Collaboration for allowing us to use their interpolation routines. A.N.K. thanks Johannes Blümlein for useful discussions, and is grateful to A. L. Kataev for the suggestion of the Jacobi polynomial method, the CERN TH-PH division for the hospitality where a portion of this work was performed, and Semnan University for financial support. We acknowledge financial support of the the School of Particles and Accelerators, Institute for Research in Fundamental Sciences (IPM). This work was partially supported by the U.S. Department of Energy under grant DE-FG02-04ER41299, and the Lightner-Sams Foundation.

Appendix: FORTRAN-code

A FORTRAN package containing our $g_1(x, Q^2)$ polarized structure functions for $\{p, n, d, NS, {}^3\text{He}, {}^3\text{H}\}$ and $xg_2^p(x, Q^2)$, as well as the polarized parton densities $\{u_v, d_v, g, \bar{q}\}$. $x\delta u_v(x, Q^2)$, $x\delta d_v(x, Q^2)$, $x\delta g(x, Q^2)$ and $x\delta \bar{q}(x, Q^2)$ at NLO in the $\overline{\text{MS}}$ -scheme can be found in <http://particles.ipm.ir/links/QCD.htm> or obtained via e-mail from the authors. These functions are interpolated using cubic splines in Q^2 and a linear interpolation in $\log(Q^2)$. The package includes an example program to illustrate the use of the routines.

[1] X. Zheng et al., The JLAB Hall A collaboration, Phys. Rev. **C70** (2004) 065207.

[2] K. V. Dharmawardane *et al.* [CLAS Collaboration], Phys. Lett. B **641** (2006) 11 [arXiv:nucl-ex/0605028].

- [3] J. Ashman *et al.* [European Muon Collaboration], Phys. Lett. B **206** (1988) 364; J. Ashman *et al.* [European Muon Collaboration], Nucl. Phys. B **328** (1989) 1.
- [4] P. L. Anthony *et al.* [E142 Collaboration], Phys. Rev. D **54** (1996) 6620 [arXiv:hep-ex/9610007].
- [5] K. Ackerstaff *et al.* [HERMES Collaboration], Phys. Lett. B **404** (1997) 383 [arXiv:hep-ex/9703005], A. Airapetian *et al.* [HERMES Collaboration], Phys. Lett. B **442** (1998) 484 [arXiv:hep-ex/9807015].
- [6] K. Abe *et al.* [E154 Collaboration], Phys. Lett. B **405** (1997) 180 [arXiv:hep-ph/9705344].
- [7] K. Abe *et al.* [E154 Collaboration], Phys. Rev. Lett. **79** (1997) 26 [arXiv:hep-ex/9705012].
- [8] B. Adeva *et al.* [Spin Muon Collaboration], Phys. Rev. D **58** (1998) 112001.
- [9] K. Abe *et al.* [E143 collaboration], Phys. Rev. D **58** (1998) 112003 [arXiv:hep-ph/9802357].
- [10] P. L. Anthony *et al.* [E155 Collaboration], Phys. Lett. B **463** (1999) 339 [arXiv:hep-ex/9904002].
- [11] P. L. Anthony *et al.* [E155 Collaboration], Phys. Lett. B **493** (2000) 19 [arXiv:hep-ph/0007248].
- [12] A. Airapetian *et al.* [HERMES Collaboration], Phys. Rev. D **75** (2007) 012007 [arXiv:hep-ex/0609039].
- [13] M. G. Alekseev *et al.* [COMPASS Collaboration], Phys. Lett. B **690**, 466 (2010) [arXiv:1001.4654 [hep-ex]], V. Y. Alexakhin *et al.* [COMPASS Collaboration], Phys. Lett. B **647** (2007) 8 [arXiv:hep-ex/0609038].
- [14] G. Altarelli, arXiv:0907.1751 [hep-ph].
- [15] M. Anselmino, A. Efremov and E. Leader, Phys. Rept. **261** (1995) 1 [Erratum-ibid. **281** (1997) 399] [arXiv:hep-ph/9501369].
- [16] B. Lampe and E. Reya, Phys. Rept. **332** (2000) 1 [arXiv:hep-ph/9810270].
- [17] E. W. Hughes and R. Voss, Ann. Rev. Nucl. Part. Sci. **49** (1999) 303.
- [18] B. W. Filippone and X. D. Ji, Adv. Nucl. Phys. **26** (2001) 1 [arXiv:hep-ph/0101224].
- [19] G. Altarelli, R. D. Ball, S. Forte and G. Ridolfi, Acta Phys. Polon. B **29** (1998) 1145 [arXiv:hep-ph/9803237].
- [20] R. D. Ball, G. Ridolfi, G. Altarelli and S. Forte, arXiv:hep-ph/9707276.
- [21] C. Bourrely, F. Buccella, O. Pisanti, P. Santorelli and J. Soffer, Prog. Theor. Phys. **99** (1998) 1017 [arXiv:hep-ph/9803229].
- [22] D. de Florian, O. A. Sampayo and R. Sassot, data,” Phys. Rev. D **57** (1998) 5803 [arXiv:hep-ph/9711440].
- [23] L. E. Gordon, M. Goshtasbpour and G. P. Ramsey, Phys. Rev. D **58** (1998) 094017 [arXiv:hep-ph/9803351].
- [24] E. Leader, A. V. Sidorov and D. B. Stamenov, Phys. Lett. B **462** (1999) 189 [arXiv:hep-ph/9905512]; E. Leader, A. V. Sidorov and D. B. Stamenov, Phys. Lett. B **445** (1998) 232 [arXiv:hep-ph/9808248], E. Leader, A. V. Sidorov and D. B. Stamenov, Phys. Rev. D **58** (1998) 114028 [arXiv:hep-ph/9807251]; E. Leader, A. V. Sidorov and D. B. Stamenov, Int. J. Mod. Phys. A **13** (1998) 5573 [arXiv:hep-ph/9708335].
- [25] M. Stratmann, Nucl. Phys. Proc. Suppl. **79** (1999) 538 [arXiv:hep-ph/9907465].
- [26] D. K. Ghosh, S. Gupta and D. Indumathi, Phys. Rev. D **62** (2000) 094012 [arXiv:hep-ph/0001287].
- [27] D. de Florian and R. Sassot, Phys. Rev. D **62** (2000) 094025 [arXiv:hep-ph/0007068].
- [28] M. Gluck, E. Reya, M. Stratmann and W. Vogelsang, Phys. Rev. D **63** (2001) 094005 [arXiv:hep-ph/0011215].
- [29] R. S. Bhaller, Phys. Rev. C **63** (2001) 025208 [arXiv:hep-ph/0003075].
- [30] E. Leader, A. V. Sidorov and D. B. Stamenov, Eur. Phys. J. C **23** (2002) 479 [arXiv:hep-ph/0111267].
- [31] J. Blumlein and H. Bottcher, Nucl. Phys. B **636** (2002) 225 [arXiv:hep-ph/0203155].
- [32] Y. Goto *et al.* [Asymmetry Analysis collaboration], Phys. Rev. D **62** (2000) 034017 [arXiv:hep-ph/0001046]; M. Hirai, S. Kumano and N. Saito [Asymmetry Analysis Collaboration], Phys. Rev. D **69** (2004) 054021 [arXiv:hep-ph/0312112].
- [33] D. de Florian, G. A. Navarro and R. Sassot, Phys. Rev. D **71** (2005) 094018 [arXiv:hep-ph/0504155].
- [34] E. Leader, A. V. Sidorov and D. B. Stamenov, Phys. Rev. D **73** (2006) 034023 [arXiv:hep-ph/0512114].
- [35] C. Bourrely, J. Soffer and F. Buccella, “A statistical approach for polarized parton distributions,” Eur. Phys. J. C **23** (2002) 487 [arXiv:hep-ph/0109160].
- [36] G. Altarelli *et al.*, Nucl. Phys. **B496** (1997) 337; Acta Phys. Pol. **B29** (1998) 1145; S. Forte, M. Mangano, and G. Ridolfi, Nucl. Phys. **B602** (2001) 585.
- [37] G. Altarelli, R. D. Ball, S. Forte and G. Ridolfi, “Determination of the Bjorken sum and strong coupling from polarized structure functions,” Nucl. Phys. B **496** (1997) 337 [arXiv:hep-ph/9701289].
- [38] D. de Florian, R. Sassot, M. Stratmann and W. Vogelsang, Phys. Rev. Lett. **101**, 072001 (2008) [arXiv:0804.0422 [hep-ph]].
- [39] M. Hirai and S. Kumano [Asymmetry Analysis Collaboration], Nucl. Phys. B **813**, 106 (2009) [arXiv:0808.0413 [hep-ph]].
- [40] J. Blumlein and H. Bottcher, arXiv:1005.3113 [hep-ph].
- [41] E. Leader, A. V. Sidorov and D. B. Stamenov, arXiv:1007.4781 [hep-ph].
- [42] J. Blumlein and H. Bottcher, arXiv:1007.2784 [hep-ph].
- [43] A. N. Khorramian, A. Mirjalili and S. A. Tehrani, JHEP **0410** (2004) 062 [arXiv:hep-ph/0411390].
- [44] S. Atashbar Tehrani and A. N. Khorramian, JHEP **0707**, 048 (2007) [arXiv:0705.2647 [hep-ph]].
- [45] G. Parisi and N. Surlas, Nucl. Phys. **B151** (1979) 421; I. S. Barker, C. B. Langensiepen and G. Shaw, Nucl. Phys. **B186** (1981) 61.
- [46] I. S. Barker, B. R. Martin and G. Shaw, Z. Phys. **C19** (1983) 147; I. S. Barker and B. R. Martin, Z. Phys. **C24** (1984) 255; S. P. Kurlovich, A. V. Sidorov and N. B. Skachkov, JINR Report E2-89-655, Dubna, 1989.
- [47] V. G. Krivokhizhin, S. P. Kurlovich, V. V. Sanadze, I. A. Savin, A. V. Sidorov and N. B. Skachkov, Z. Phys. C **36** (1987) 51.
- [48] V. G. Krivokhizhin *et al.*, Z. Phys. C **48**, 347 (1990).
- [49] J. Chyla and J. Rames, Z. Phys. C **31** (1986) 151.
- [50] I. S. Barker, C. S. Langensiepen and G. Shaw, Nucl. Phys. B **186** (1981) 61.
- [51] A. L. Kataev, A. V. Kotikov, G. Parente and A. V. Sidorov, Phys. Lett. B **417**, (1998) 374 [arXiv:hep-ph/9706534].
- [52] A. L. Kataev, G. Parente and A. V. Sidorov, arXiv:hep-ph/9809500.
- [53] A. L. Kataev, G. Parente and A. V. Sidorov, Nucl. Phys. B **573**, (2000) 405 [arXiv:hep-ph/9905310].
- [54] A. L. Kataev, G. Parente and A. V. Sidorov, Phys. Part. Nucl. **34**, (2003) 20 [arXiv:hep-ph/0106221];

- A. L. Kataev, G. Parente and A. V. Sidorov, Nucl. Phys. Proc. Suppl. **116** (2003) 105 [arXiv:hep-ph/0211151].
- [55] A. N. Khorramian, S. Atashbar Tehrani and M. Ghominejad, Acta Phys. Polon. B **38**, 3551 (2007).
- [56] A. N. Khorramian and S. A. Tehrani, J. Phys. Conf. Ser. **110**, 022022 (2008).
- [57] A. N. Khorramian and S. A. Tehrani, AIP Conf. Proc. **1006** (2008) 118.
- [58] S. Atashbar Tehrani and A. N. Khorramian, Nucl. Phys. Proc. Suppl. **186**, 58 (2009).
- [59] A. N. Khorramian, S. Atashbar Tehrani, H. Khanpour and S. Taheri Monfared, Hyperfine Interactions **194**, 337 (2009).
- [60] A. N. Khorramian, S. Atashbar Tehrani, M. Soleymaninia. and S. Batebi, Hyperfine Interactions **194**, 341 (2009).
- [61] S. Atashbar Tehrani and A. N. Khorramian, Hyperfine Interactions **194**, 331 (2009).
- [62] S. Atashbar Tehrani and A. N. Khorramian, Applied Mathematics & Information Sciences (2009), 367-373.
- [63] A. N. Khorramian and S. A. Tehrani, Phys. Rev. D **78**, 074019 (2008) [arXiv:0805.3063 [hep-ph]].
- [64] A. N. Khorramian, H. Khanpour and S. Atashbar Tehrani, PoS EPS-HEP2009, 393 (2009).
- [65] H. Khanpour, A. N. Khorramian, S. Atashbar Tehrani and A. Mirjalili, Acta Phys. Polon. B **40**, 2971 (2009).
- [66] A. N. Khorramian, H. Khanpour and S. A. Tehrani, Phys. Rev. D **81**, 014013 (2010) [arXiv:0909.2665 [hep-ph]].
- [67] E. Leader, A. V. Sidorov and D. B. Stamenov, Int. J. Mod. Phys. A **13**, 5573 (1998) [arXiv:hep-ph/9708335].
- [68] Ali. N. Khorramian, S. Atashbar Tehrani, F. Olness, S. Taheri Monafred, F. Arbabifar, Nucl. Phys. Proc. Suppl. **207**, 65 (2010); F. Arbabifar, Ali. N. Khorramian, S. Atashbar Tehrani, A. Najafgholi, Proceedings of the Conference in Honor of Murray Gell-Mann's 80th Birthday, World Scientific, 503-510 (2010).
- [69] A. Mirjalili, A. N. Khorramian, S. Atashbar Tehrani and H. Mahdizadeh Saffar, Acta Phys. Polon. B **40**, 2965 (2009).
- [70] A. N. Khorramian and S. Atashbar Tehrani, arXiv:0712.2373 [hep-ph].
- [71] A. N. Khorramian and S. Atashbar Tehrani, AIP Conf. Proc. **915**, 420 (2007).
- [72] A. Mirjalili, A. N. Khorramian and S. Atashbar-Tehrani, Nucl. Phys. Proc. Suppl. **164**, 38 (2007).
- [73] A. Mirjalili, S. Atashbar Tehrani and A. N. Khorramian, Int. J. Mod. Phys. A **21**, 4599 (2006) [arXiv:hep-ph/0608224].
- [74] C. Amsler et al. (Particle Data Group), Phys. Lett. B **667** (2008) 1.
- [75] A. Vogt, Comput. Phys. Commun. **170**, 65 (2005) [arXiv:hep-ph/0408244].
- [76] D. Stump *et al.*, Phys. Rev. D **65**, 014012 (2002) [arXiv:hep-ph/0101051].
- [77] M. Lacombe, B. Loiseau, R. Vinh Mau, J. Cote, P. Pires and R. de Tourreil, Phys. Lett. B **101** (1981) 139; W. W. Buck and F. Gross, Phys. Rev. D **20** (1979) 2361; M. J. Zuilhof and J. A. Tjon, Phys. Rev. C **22** (1980) 2369; R. Machleidt, K. Holinde and C. Elster, Phys. Rept. **149** (1987) 1; A. Y. Umnikov, L. P. Kaptari, K. Y. Kazakov and F. C. Khanna, arXiv:hep-ph/9410241.
- [78] S. Wandzura and F. Wilczek, Phys. Lett. B **72**, 195 (1977).
- [79] A. Piccione and G. Ridolfi, Nucl. Phys. B **513**, 301 (1998) [arXiv:hep-ph/9707478].
- [80] J. Blümlein, H. Böttcher and A. Guffanti, Nucl. Phys. B **774** (2007) 182 [arXiv:hep-ph/0607200]; Nucl. Phys. Proc. Suppl. **135** (2004) 152 [arXiv:hep-ph/0407089].
- [81] S. Alekhin, J. Blümlein, S. Klein and S. Moch, Phys. Rev. D **81** (2010) 014032 [arXiv:0908.2766 [hep-ph]].
- [82] M. Glück, E. Reya and C. Schuck, Nucl. Phys. B **754** (2006) 178 [arXiv:hep-ph/0604116]; P. Jimenez-Delgado and E. Reya, Phys. Rev. D **79** (2009) 074023 [arXiv:0810.4274 [hep-ph]].
- [83] A. D. Martin, W. J. Stirling, R. S. Thorne and G. Watt, Eur. Phys. J. C **64** (2009) 653 [arXiv:0905.3531 [hep-ph]].
- [84] S.I. Alekhin, J. Blümlein, and S.-O. Moch, DESY 10-065, in preparation.
- [85] H1 and ZEUS collab. (V. Radescu et al.), Combined H1 and ZEUS Fits Using Low Energy Data, talk, DIS 2010, Florence, April 2010; F. D. Aaron *et al.* [H1 Collaboration and ZEUS Collaboration], JHEP **1001** (2010) 109 [arXiv:0911.0884 [hep-ex]].
- [86] S. Bethke, arXiv:0908.1135 [hep-ph].
- [87] M. M. Yazdanpanah, A. Mirjalili, S. Atashbar Tehrani and F. Taghavi-Shahri, Nucl. Phys. A **831**, 243 (2009).
- [88] F. R. P. Bissey, V. A. Guzey, M. Strikman and A. W. Thomas, Phys. Rev. C **65**, 064317 (2002) [arXiv:hep-ph/0109069].
- [89] F. R. P. Bissey, A. W. Thomas and I. R. Afnan, Phys. Rev. C **64**, 024004 (2001) [arXiv:nucl-th/0012081].
- [90] I. R. Afnan *et al.*, Phys. Rev. C **68**, 035201 (2003) [arXiv:nucl-th/0306054].
- [91]
- [91] J. D. Bjorken, Phys. Rev. **148**, 1467 (1966).
- [92] B. Budick, J. S. Chen and H. Lin, Phys. Rev. Lett. **67**, 2630 (1991).